 CMES, vol.105, no.1, pp.25-45, 2015

A 3-D Visco-Hyperelastic Constitutive Model for Rubber with Damage for Finite Element Simulation

Ala Tabiei[1] **and Suraush Khambati**[2]

Abstract: A constitutive model to describe the behavior of rubber from low to high strain rates is presented. For loading, the primary hyperelastic behavior is characterized by the six parameter Ogden's strain-energy potential of the third order. The rate-dependence is captured by the nonlinear second order BKZ model using another five parameters, having two relaxation times. For unloading, a single parameter model has been presented to define Hysteresis or continuous damage, while Ogden's two term model has been used to capture Mullin's effect or discontinuous damage. Lastly, the Feng-Hallquist failure surface dictates the ultimate failure for element deletion. The proposed model can accurately predict the response of rubber using a limited set of experimental data. The model has been validated here for the case of rubber but can be extended to a wide range of polymers.

Keywords: hyperelasticity, viscoelasticity, hysteresis, Mullin's effect, rubber, constitutive.

Nomenclature

$\lambda_1, \lambda_2, \lambda_3$	Principal Stretches
W	Strain-energy potential
μ_1, μ_2, μ_3	Material Constants (Shear moduli) for Ogden's Strain-energy potential
$\alpha_1, \alpha_2, \alpha_3$	Material Constants (Exponents) for Ogden's Strain-energy potential
G	Shear Modulus
σ	Cauchy's stress tensor
F	Deformation gradient
dx	Infinitesimal material element in deformed configuration
dX	Infinitesimal material element in reference configuration

[1] Associate Professor. School of Advance Structures, College of Engineering and Applied Sciences, University of Cincinnati, OH 45221-0071, USA. E-mail: ala.tabiei@uc.edu

[2] Graduate Student. School of Advance Structures, College of Engineering and Applied Sciences, University of Cincinnati, OH 45221-0071, USA. E-mail: khambasq@mail.uc.edu

J	Jacobian
C	Right Cauchy-Green deformation tensor
$\dot{C}$	Rate of Change of Right Cauchy-Green deformation tensor
$\dot{F}$	Rate of Change of Deformation gradient
P	1^{st} Piola-Kirchhoff stress
S	2^{nd} Piola-Kirchhoff stress
p	Hydrostatic pressure
c	Constant for pure homogenous deformation
σ^h	Hyperelastic component of Cauchy's stress tensor
σ^v	Viscoelastic component of Cauchy's stress tensor
p^v	Pressure in viscoelastic material
Ω	Matrix function
t	Time
τ	Time integral
φ	Function of invariants of Right Cauchy-Green deformation tensor
I_1, I_2, I_3	Invariants of Right Cauchy-Green deformation tensor
M	Relaxation function
$\dot{E}$	Strain rate
θ_1, θ_2	Relaxation times
$\dot{\lambda}$	Strain rate
C_1, C_2, C_3	Viscoelastic constants (in function of invariants)
C_4, C_5	Viscoelastic constants (relaxation times)
S	Stretch Integral
$\phi(\eta)$	Function of Damage
η	Damage variable
α	Damage parameter
λ_m	Maximum stretch at which unloading starts
P_u	Unloading value of 1^{st} Piola-Kirchhoff stress
W_O	Primary Strain-energy potential
r, m	Material constants for Mullins' effect
erf	Error function
W_m	Strain-energy potential at maximum stretch
η_m	Minimum value of damage variable (at complete unloading)
ϕ_{mullins}	Damage due to Mullins' effect
$\phi_{\text{hysteresis}}$	Damage due to hysteresis
Ψ	Failure criteria
β	Constant for Feng-Hallquist failure surface
Γ_1, Γ_2, K	Material failure constants

1 Introduction

Rubber is commonly used in automotives as tires, transmission belts, hoses, gaskets, seals, vibration isolation mounts, interlayer in windshields, and in architectural applications as transparent armor and ballistic protection. Thus, depending on the intensity and frequency of the load, rubber exhibits deformation over a range of strain-rates varying from low to high. Due to their hyperelastic nature, rubber-like polymers can withstand large strains without undergoing permanent deformation, hence providing large energy absorption. Therefore, it is necessary to have a constitutive model that can incorporate its' various characteristics including rate-sensitivity, creep, relaxation, hysteresis and Mullin's effect.

Here, a phenomenological stretched-based constitutive model has been developed for rubber, which is consistent within the laws of continuum mechanics and theories of deformation. The mathematical formulation of new and existing models has been presented toward developing one unified model. The various sections which this study focuses on, can be summarized as follows:

1. Hyperelasticity – Ogden's hyperelastic strain energy potential of the third order was used to characterize the primary material response, i.e. hyperelasticity [Ogden (1972)].

2. Viscoelasticity – the viscoelastic component of the Cauchy's stress is given by the BKZ model [Zapas (1966)] of order two – implying two relaxation times – each corresponding to low strain rates of 10^{-4} mm/mm/s to 10^{-1}mm/mm/s and high strain rates of 10^{2} mm/mm/s to 10^{3} mm/mm/s.

3. Hysteresis – intended for modeling large-strain rate-dependent behavior of elastomers. Here the corresponding primary foam behavior is scaled by the damage variable to provide the unloading response. It is a continuous type of damage.

4. Mullins' effect – is used for modeling the stress softening of filled elastomers (like rubber) under quasi-static loading. The material requires less stress on reloading than initial loading for stretches up to maximum stretch during initial loading. This stress softening behavior is called as Mullins effect and it reflects the damage incurred during previous loading cycles [Mullins (1969)]. The energy required to cause damage is not recoverable. Damage occurs at microscopic level by severing bonds between filler particles and rubber molecular chains. It is a discontinuous type of damage.

5. Failure Surface – The Feng-Hallquist failure surface has been studied and suggested as a suitable model wherein data from stretch-to-failure experi-

mental tests is required to completely characterize the model and obtain material parameters [Feng (2007)].

In what follows, each of the above mentioned topics is presented and discussed in detail.

2 Constitutive Model

2.1 Hyperelasticity

A hyperelastic material is a type of constitutive model for ideal elastic materials for which the stress-strain relationship is derived from a strain-energy density function. In this particular section, we assume the hyperelastic response as non-linear elastic, isotropic, incompressible and independent of strain-rate.

Ogden developed a sophisticated way for simulating incompressible (rubber-like) materials like biological soft tissues and solid polymers which undergo finite strains relative to an equilibrium state in the phenomenological context [Ogden (1972)]. The postulated strain energy is a function of the principal stretches λ_a, a = 1, 2, 3. The Ogden hyperelastic strain energy potential is given by

$$\mathrm{W} = \sum_{\mathrm{n}=1}^{3} \frac{\mu_n}{\alpha_n}[\lambda_1^{\alpha_n} + \lambda_2^{\alpha_n} + \lambda_3^{\alpha_n} - 3] \tag{1}$$

where $\sum\limits_{\mathrm{n}=1}^{3} \mu_n, \alpha_n$ are the material coefficients.

The conventional Shear Modulus G (in the undeformed, stress-free or natural configuration) is given by

$$\mathrm{G} = \sum_{\mathrm{n}=1}^{3} \mu_n \alpha_n \tag{2}$$

For incompressible materials,

$$\lambda_1 \lambda_2 \lambda_3 = 1 \tag{3}$$

Now, in order to obtain stress in terms of the strain-energy potential, let's state a few important relationships. Internal forces are represented by Cauchy's stress tensor σ and F is the deformation gradient. The deformation gradient F is given by [Holzapfel (2000) and Hutter (1993)]:

$$\mathrm{F} = \frac{\delta x}{\delta X} \tag{4}$$

with the Jacobian, $\mathrm{J} = \det(\mathrm{F})$, which is the ratio of volumes in current and deformed configurations.
The right Cauchy-Green deformation tensor is defined in terms of F as

$$\mathrm{C} = \mathrm{F}^{T}\mathrm{F} \tag{5}$$

The rate of change of the right Cauchy-Green deformation tensor is given as [Hutter (1993) and Bower (2009)]

$$\dot{\mathrm{C}} = \dot{\mathrm{F}}^{\mathrm{T}}\mathrm{F} + \mathrm{F}^{\mathrm{T}}\dot{\mathrm{F}} \tag{6}$$

In terms of the 1^{st} Piola-Kirchhoff stress:

$$\mathrm{P} = \sigma J F^{-1} \tag{7}$$

In terms of the 2^{nd} Piola-Kirchhoff stress:

$$\mathrm{S} = \mathrm{J}\mathrm{F}^{-1}\sigma F^{-T} \tag{8}$$

Now, we can write the Cauchy's stress in terms of the strain-energy potential as

$$\sigma_i = \frac{1}{\lambda_j\lambda_k}\frac{\delta W}{\delta\lambda_i} - \mathrm{p} \tag{9}$$

where p is the hydrostatic pressure.
The first Piola-Kirchoff Stress (1^{st} PK) is

$$\mathrm{P}_i = \frac{\sigma_i}{\lambda_i} \tag{10}$$

The following cases of principal stretch values λ_a, a = 1, 2, 3, in terms of stretch in the primary direction λ, are particularly useful while using experimental data:

$$\text{For Simple Tension,} \quad \lambda_1 = \lambda,\ \lambda_2 = \lambda_3 = \lambda^{-\frac{1}{2}} \tag{11}$$

$$\text{For Pure Shear,} \quad \lambda_1 = \lambda,\ \lambda_2 = 1,\ \lambda_3 = \lambda^{-1} \tag{12}$$

$$\text{For Equibiaxial Tension,} \quad \lambda_1 = \lambda_2 = \lambda,\ \lambda_3 = \lambda^{-2} \tag{13}$$

The material constants $\sum\limits_{\mathrm{n}=1}^{3} \mu_n, \alpha_n$ and the stress-deformation function is given as [Ogden (2004)]:

$$\mathrm{P} = \sum_{\mathrm{n}=1}^{3} \mu_n[\lambda^{-1+\alpha_n} - \lambda^{-1+c\alpha_n}] \tag{14}$$

where P = Force per unit undeformed area or 1^{st} PK stress,
c = Pure homogeneous deformation.
For simple tension $c = -1/2$,
For pure shear $c = -1$, and,
For equi-biaxial tension $c = -2$.

2.2 Viscoelasticity

A real system exhibits behavior which is a combination of solid and liquid like characteristics. Some of the energy input is stored and recovered in each cycle while some is dissipated as heat. Such materials are called viscoelastic. If both strain and stress are infinitesimal, then the body exhibits linear viscoelasticity [Ferry (1961)]. The overall response of the material can thus be written as: $\sigma = \sigma^h + \sigma^v$.

The viscoelastic component as given by the BKZ Model [Bernstein (1963), Bernstein (1965) and Yang (2004)] is:

$$\sigma^v = -\mathrm{p}^v + \mathrm{F}(\mathrm{t})\,\Omega^t_{\tau=-\infty}\{\mathrm{C}(\tau)\}\,\mathrm{F}^t(\mathrm{t}) \tag{15}$$

where p^v is the pressure in the viscoelastic material.
The matrix function is:

$$\Omega^{\mathrm{t}}_{\tau=-\infty}\{\mathrm{C}(\tau)\} = \int_{-\infty}^{\mathrm{t}} \phi(\mathrm{I}_1,\mathrm{I}_2)\,\mathrm{M}(\mathrm{t}-\tau)\,\dot{\mathrm{E}}(\tau)\,\mathrm{d}\tau \tag{16}$$

The strain rate is given by the following equation:

$$\dot{\mathrm{E}} = \frac{1}{2}\left(\dot{\mathrm{F}}^{\mathrm{T}}\mathrm{F} + \mathrm{F}^{\mathrm{T}}\dot{\mathrm{F}}\right) \tag{17}$$

And the relaxation function is:

$$\mathrm{M} = \sum_{\mathrm{i}=1}^{N} \exp\left(-\frac{\mathrm{t}-\tau}{\theta_i}\right) \tag{18}$$

where θ_i is the relaxation time. We consider $\mathrm{N} = 2$, following the BKZ model:
θ_1 corresponds to low strain rates of 10^{-4} to 10^{-1} mm/mm/s
θ_2 corresponds to high strain rates of 10^2 to 10^3 mm/mm/s
Once we obtain the hyperelastic constants, we can find the viscoelastic constants next. Here, taking the strain rate 0.01 mm/mm/s assuming it to be quasi-static, we use the six hyperelastic constants to characterize the quasi-static response. For the

case of uniaxial extension, we have the deformation gradient as [Yang (2004) and Yang (2000)]:

$$\mathrm{F}=\begin{bmatrix}\lambda & 0 & 0\\ 0 & \lambda^{-\frac{1}{2}} & 0\\ 0 & 0 & \lambda^{-\frac{1}{2}}\end{bmatrix} \tag{19}$$

$$\begin{aligned}\text{Since}\quad & \mathrm{F}^{t}_{11}=\mathrm{F}_{11}=\lambda,\quad \mathrm{F}^{t}_{22}=\mathrm{F}_{22}=\lambda^{-\frac{1}{2}},\quad \mathrm{F}^{t}_{33}=\mathrm{F}_{33}=\lambda^{-\frac{1}{2}}\\ & \dot{\mathrm{F}}_{11}=\dot{\lambda},\quad \dot{\mathrm{F}}_{22}=-\frac{1}{2}\lambda^{-\frac{3}{2}}\dot{\lambda},\quad \dot{\mathrm{F}}_{33}=-\frac{1}{2}\lambda^{-\frac{3}{2}}\dot{\lambda}\end{aligned} \tag{20}$$

Also, the invariants of the right Cauchy-Green deformation tensor are given by:

$$\begin{aligned}\mathrm{I}_1&=\lambda_1^2+\lambda_2^2+\lambda_3^2=\lambda^2+2\lambda^{-1}\\ \mathrm{I}_2&=\lambda_2^2\lambda_3^2+\lambda_3^2\lambda_1^2+\lambda_1^2\lambda_2^2=\lambda^{-2}+2\lambda\dot{\lambda}\end{aligned} \tag{21}$$

In equation (16) and (18), $\mathrm{t}-\tau$ is the amount of time that has elapsed between τ and t, so we consider contributions from all $\tau<\mathrm{t}$ [Silva (2008)]. Thus, effect of deformation history on stress for $\tau<0$ at time $\mathrm{t}>0$ is ignored.
Redefining the integration limits in terms of stretch:

$$\dot{\lambda}=\frac{\mathrm{d}\lambda}{\mathrm{dt}}\rightarrow\int_0^{\mathrm{t}}\mathrm{dt}=\int_1^{\lambda}\frac{1}{\dot{\lambda}}\mathrm{d}\lambda\rightarrow\mathrm{t}=\frac{\lambda-1}{\dot{\lambda}} \tag{22}$$

In equation (15) for σ^{v}, we assume the following form for ϕ,

$$\phi=\phi_1=\phi_2=\mathrm{C}_1\mathrm{I}_1+\mathrm{C}_2\mathrm{I}_2+\mathrm{C}_3 \tag{23}$$

Since the relaxation times θ_1 and θ_2 are constants, they will be referred to as C_4 and C_5 respectively. Thus, we can write the viscoelastic component of stress at time t, by substituting (16) (17) (18) and (23) in equation (15), as

$$\sigma^{\mathrm{v}}=-\mathrm{p}^{\mathrm{v}}+\mathrm{F}\left\{\int_0^{\mathrm{t}}\phi_1\exp\left(-\frac{\mathrm{t}-\tau}{\mathrm{C}_4}\right)\dot{\mathrm{E}}(\tau)\,\mathrm{d}\tau+\int_0^{\mathrm{t}}\phi_2\exp\left(-\frac{\mathrm{t}-\tau}{\mathrm{C}_5}\right)\dot{\mathrm{E}}(\tau)\,\mathrm{d}\tau\right\}\mathrm{F}^{\mathrm{T}} \tag{24}$$

Where the strain-rate from (17) and (19) is

$$\begin{aligned}\dot{\mathrm{E}}_{11}&=\frac{1}{2}\left(\dot{\lambda}\lambda+\lambda\dot{\lambda}\right)=\lambda\dot{\lambda}\\ \dot{\mathrm{E}}_{22}=\dot{\mathrm{E}}_{33}&=\frac{1}{2}\left[\left(\lambda^{-\frac{1}{2}}\right)\left(-\frac{1}{2}\lambda^{-\frac{3}{2}}\right)\left(\dot{\lambda}\right)-\left(\frac{1}{2}\lambda^{-\frac{3}{2}}\right)\left(\dot{\lambda}\right)\left(\lambda^{-\frac{1}{2}}\right)\right]=-\frac{1}{2}\lambda^{-2}\dot{\lambda}\end{aligned} \tag{25}$$

Since t is a constant for integration and τ is a time variable, we can rewrite (21) in terms of its' principal components as

$$\begin{aligned}
&\sigma_{11}{}^{\mathrm{v}} = -\mathrm{p}^{\mathrm{v}} + \lambda^2 \left\{ \int_0^{\mathrm{t}} \phi_1 \exp\left(-\frac{\mathrm{t}-\tau}{\mathrm{C}_4}\right) \lambda\dot{\lambda}\mathrm{d}\tau + \int_0^{\mathrm{t}} \phi_2 \exp\left(-\frac{\mathrm{t}-\tau}{\mathrm{C}_5}\right) \lambda\dot{\lambda}\mathrm{d}\tau \right\} \\
&\sigma_{22}{}^{\mathrm{v}} = \sigma_{33}{}^{\mathrm{v}} = 0 = -\mathrm{p}^{\mathrm{v}} + \lambda^{-1} \left\{ \begin{array}{l} \int_0^{\mathrm{t}} \phi_1 \exp\left(-\frac{\mathrm{t}-\tau}{\mathrm{C}_4}\right) \left(-\frac{1}{2}\lambda^{-2}\dot{\lambda}\right) d\tau + \\ \int_0^{\mathrm{t}} \phi_2 exp\left(-\frac{\mathrm{t}-\tau}{\mathrm{C}_5}\right) \left(-\frac{1}{2}\lambda^{-2}\dot{\lambda}\right) d\tau \end{array} \right\}
\end{aligned} \tag{26}$$

Substituting the value for p^v in the above equations in (26), we get equation (27) as follows, which we curve fit to experimental data:

$$\begin{aligned}
\sigma_{11}{}^{v} =& \frac{1}{2}\lambda^{-1} \Big\{ \int_0^t (C_1 I_1 + C_2 I_2 + C_3) \exp\left(-\frac{t-\tau}{C_4}\right) \left(\lambda^{-2}\dot{\lambda}\right) d\tau \\
&+ \int_0^t (C_1 I_1 + C_2 I_2 + C_3) \exp\left(-\frac{t-\tau}{C_5}\right) \left(\lambda^{-2}\dot{\lambda}\right) d\tau \Big\} \\
&+ \lambda^2 \Big\{ \int_0^t (C_1 I_1 + C_2 I_2 + C_3) \exp\left(-\frac{t-\tau}{C_4}\right) \left(\lambda\dot{\lambda}\right) d\tau \\
&+ \int_0^t (C_1 I_1 + C_2 I_2 + C_3) \exp\left(-\frac{t-\tau}{C_5}\right) \left(\lambda\dot{\lambda}\right) d\tau \Big\}
\end{aligned} \tag{27}$$

While τ ranges from $(0,\mathrm{t})$, the stretch integral S ranges from $(1,\lambda)$, thus we can write:

$$\begin{aligned}
&\tau = 0, \quad \mathrm{S} = 1 \\
&\tau = \mathrm{t}, \quad \mathrm{S} = \lambda
\end{aligned} \tag{28}$$

where t corresponds to final stretch λ, while τ corresponds to current stretch S. Thus, in the curve fitting equation (27) for σ_{11}^v, we substitute all values of λ by S in the curly parentheses $\{\}$, because it is a variable to be integrated between $(0,\mathrm{t})$ or $(1,\lambda)$.

Since in our case we have data at three different strain rates, we can determine the σ_1^v, σ_2^v, σ_3^v, or the viscoelastic stress components for the three test curves. Thus, for each of the curves, we can get the hyperelastic component of stress by subtracting each viscoelastic stress component from the test curve as $\sigma_i^h = \sigma_i - \sigma_i^v$. The three new curves σ_i^h should almost superimpose into a single curve, in order to validate the correctness of the model.

2.3 Hysteresis

Filled elastomers exhibit dissipative properties leading to hysteresis in cyclic load-strain curves due to chain-breakage, micro-structural damage and micro-void formation. In other words, since some energy is lost or dissipated as heat, they require more energy during loading than upon unloading. A stretch-based framework is proposed for modeling the continuum damage behavior of rubber and to simulate fatigue behavior.

Hysteresis is intended for modeling large-strain rate-dependent behavior of elastomers. Energy dissipation through hysteresis is represented by the area between the loading and unloading curves in a load-deformation cycle, and occurs in all types of rubber. The complementary property of hysteresis is resilience, which is a measure of the energy returned during each cycle.

The augmented energy potential is given [Dorfmann (2003)] as:

$$\mathrm{W}(\lambda,\eta) = (1-\eta)\,\mathrm{W}(\lambda) + \phi(\eta) \tag{29}$$

where $\mathrm{W}(\lambda)$ is the strain-energy potential during loading and η is the damage variable.

At $\eta = 0$, no damage occurs and $\mathrm{W}(\lambda,0) = \mathrm{W}(\lambda)$ or the primary curve is followed.

The Cauchy's stress is given by

$$\sigma(\eta,\lambda) = (1-\eta)\,\sigma(\lambda) \tag{30}$$

where $\sigma(\lambda)$ corresponds to primary foam behavior, scaled by the damage variable $(1-\eta)$.

Next, to define the damage variable η [Calvo (2009)], we employ a stretch-based form as given below:

$$\eta = \frac{\lambda - \lambda_m}{\alpha - \lambda_m} \tag{31}$$

where λ_m is the maximum value of λ during the deformation history and α is a dimensionless material parameter.

The energy dissipated due to damage in the material is given by $\phi(\eta_m)$, and the recoverable part of energy is given by:

$$(1-\eta)\,\mathrm{W}(\lambda) + \phi(\eta) - \phi(\eta_m) \tag{32}$$

Now, for computing the damage parameter α for unloading during an experiment, say uniaxial hyperelastic extension, we first find the hyperelastic constants as described earlier. Next we separate the data into the tensile and compressive zones for the unloading curve.

Now, starting off with the tensile curve, we find the maximum stretch on the loading curve, call it *max*. Then for every data point on the unloading curve, say, *current* stretch we compute the 1^{st} PK stress as:

$$\mathrm{P} = \sum_{\mathrm{n}=1}^{3} \mu_n \left[\lambda^{-1+\alpha_n} - \lambda^{-1-\frac{1}{2}\alpha_n}\right] \tag{33}$$

As in (30), we compute the unloading stress value by scaling it by $(1-\eta)$ as follows:

$$\mathrm{P}_u = (1-\eta)\,\mathrm{P} \tag{34}$$

2.4 Mullins' effect

Mullins effect is used for modeling the stress softening of filled rubber-like elastomers under quasi-static loading [Mullins (1969) and Dorfmann (2003)]. Elastomers soften significantly when exercised and this strain softening is most pronounced between the first and second cycles, then usually disappearing between the third and fourth cycles. Thus, Mullins' effect is a discontinuous type of damage evolution.

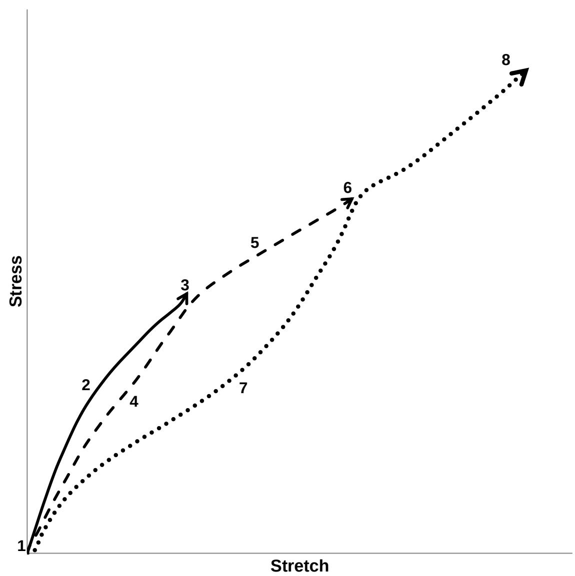

Figure 1: Mullins' effect schematic representation.

Figure 1 represents Mullins' effect schematically. In the figure one can observe the following:

1. Curve 1-2-3 is the primary loading path
2. Curve 3-4-1 is the unloading path from point 3
3. Curve 1-4-3 is the reloading path upto point 3
4. Curve 3-5-6 is the reloading path beyond point 3
5. Curve 6-7-1 is the unloading path from point 6

The augmented energy potential is given by the following equation:

$$\mathrm{W}(\lambda_1, \lambda_2, \eta) = \eta W_O + \phi(\eta) \tag{35}$$

where η is the damage variable and $\phi(\eta)$ is a function of damage.

The Cauchy's stress is given by:

$$\sigma(\eta, \lambda) = \eta \sigma(\lambda) \tag{36}$$

where $\sigma(\lambda)$ corresponds to primary foam behavior, scaled by the damage variable η.

Let λ_m be the point where unloading has most recently initiated, the unloading stress at a particular stretch is given by multiplying the stress at loading by the damage variable η. Upon reloading, if $\lambda >> \lambda_m$ then $\eta = 1$, or in other words the primary load path is active after stretching beyond the maximum stretch attained in the previous loading cycles.

We assume the following form of the damage variable as proposed by Ogden-Roxburgh [Ogden (1988)]:

$$\eta = 1 - \frac{1}{\mathrm{r}} \mathrm{erf}\left\{\frac{1}{\mathrm{m}}\left[\mathrm{W}_m - \mathrm{W}(\lambda_1, \lambda_2)\right]\right\} \tag{37}$$

where r, m are positive parameters or material constants, and erf is the error function which is suitable to capture the nature of the unloading curve and is given by the following:

$$\mathrm{erf}(\mathrm{x}) = \frac{2}{\sqrt{\pi}} \int_0^x \mathrm{e}^{-\mathrm{t}^2} \mathrm{dt} \tag{38}$$

At $\lambda_1 = \lambda_2 = 1$, when the material is fully unloaded, η attains it's minimum value η_m and $\phi(\eta_m)$ is the residual (or non-recoverable energy) which gives the measure of the energy required to cause damage in the material. In a uniaxial experiment, $\phi(\eta_m)$ equals to the area between primary loading curve and relevant unloading curve.

The recoverable part of the energy is given by:

$$\mathrm{W}_m - \phi(\eta_m) \tag{39}$$

At the microscopic level, stress softening is associated with the damage caused by loading by severing the bonds between the filler particles and the rubber molecular chains.

The total damage is thus given by [Miehe (1995)]:

$$\phi = \phi_{\text{mullins}} + \phi_{\text{hysteresis}} \tag{40}$$

2.5 Failure surface

In most structural applications, the finite element method is used to predict failure. This is done by comparing the calculated solution to some failure criteria. The failure description for rubber used here is the general failure criterion for polymers as given by Feng and Hallquist [Feng (2005) and Feng (2007)]. The failure surface is based on the energy principle – when the strain energy reaches a maximum, the material fails. Although, rubber may fail when subjected to repeated applied stress cycles even when they are well below the single cycle breaking stress.

In terms of the deformation gradient F, the failure surface is given by the following:

$$\mathrm{F}\left(\mathrm{I}_1, \mathrm{I}_2, \mathrm{I}_3\right) = 0 \tag{41}$$

For incompressible materials, $\mathrm{I}_3 = 1$ and the failure surface in (38) simplifies to

$$\mathrm{F}\left(\mathrm{I}_1, \mathrm{I}_2\right) = 0 \tag{42}$$

Further expanding (42), we get the failure criterion for hyperelastic solids as

$$\Psi = \mathrm{F}_1\left(\mathrm{I}_1 - 3\right) + \mathrm{F}_{11}\left(\mathrm{I}_1 - 3\right)^2 + \mathrm{F}_2\left(\mathrm{I}_2 - 3\right) + \beta \tag{43}$$

Any strain rate satisfying $\Psi < 0$ is below the failure state and represents a stress-free state, thus $\beta < 0$ is required. Thus, failure surface is described by state in which $\beta = 0$

$$\rightarrow \left(\mathrm{I}_1 - 3\right) + \Gamma_1\left(\mathrm{I}_1 - 3\right)^2 + \Gamma_2\left(\mathrm{I}_2 - 3\right) - \mathrm{K} = 0 \tag{44}$$

where Γ_1, Γ_2 and K are the 3 material failure constants and can be obtained from test data (a minimum of three tests are required).

3 Results and Discussion

3.1 Hyperelasticity

Ogden's three-term model

For our validation, we first find the parameters for the three-term Ogden model in the following modes of deformation simultaneously: in simple tension, pure shear and equibiaxial tension. The data [Ogden (2004)] we use is given in *Figure 2*. Using the first set of values to iteratively converge at a solution such that the value of the sum of squares remains nearly constant so as to represent a stable set of values: as seen in *Table 1*. The curve fit is given by *Figure 2* which captures all three modes of deformation very accurately with the same set of material parameters, as given by *Table 2* [Twizell (1983)]. The order of stiffness is given by

$$\text{Equibiaxial Tension} >> \text{Pure Shear} >> \text{Simple Tension}$$

Table 1: Minimizing function.

μ_1	$4.2370\frac{kg}{cm^2}$	$0.0563\frac{kg}{cm^2}$	$0.001\frac{kg}{cm^2}$	$1.8976\text{E-}5\frac{kg}{cm^2}$
α_1	0.5066	4.3733	8.1036	8.1472
μ_2	$3.2263\frac{kg}{cm^2}$	$-0.0174\frac{kg}{cm^2}$	$-0.2928\frac{kg}{cm^2}$	$-0.1197\frac{kg}{cm^2}$
α_2	2.5065	-2.5641	-1.6527	-1.9574
μ_3	$-4.1551\frac{kg}{cm^2}$	$79.6349\frac{kg}{cm^2}$	$3.0879\frac{kg}{cm^2}$	$3.3553\frac{kg}{cm^2}$
α_3	1.7730	0.1038	2.0014	1.9575
S	611.7291	81.01	13.5405	$12.9052(const)$

Table 2: Material parameters obtained for Ogden model.

μ_1	μ_2	μ_3
$1.89\text{E-}5\ \frac{kg}{cm^2}$	$-0.12\ \frac{kg}{cm^2}$	$3.36\ \frac{kg}{cm^2}$
α_1	α_2	α_3
8.15	-1.96	1.96

3.2 Viscoelasticity

Quasi-static Response

In the previous section, we see that the hyperelastic model can capture deformation in various different modes. Next, we go on to evaluate the viscoelastic model for

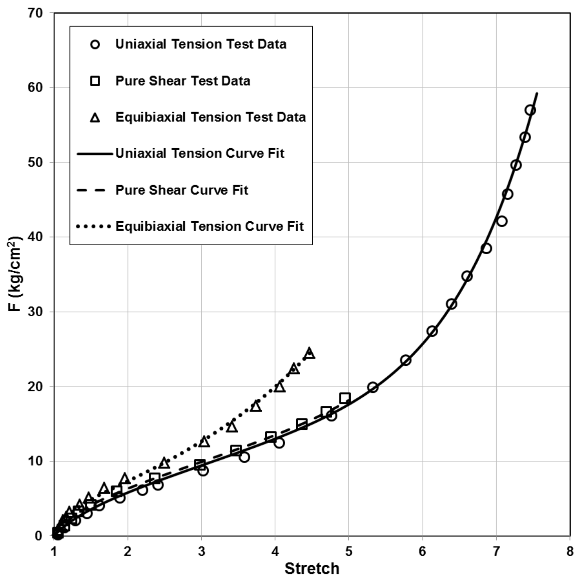

Figure 2: Experimental data [19] for 8% S rubber in uniaxial tension, pure shear and equibiaxial tension fitted to the three-term Ogden model.

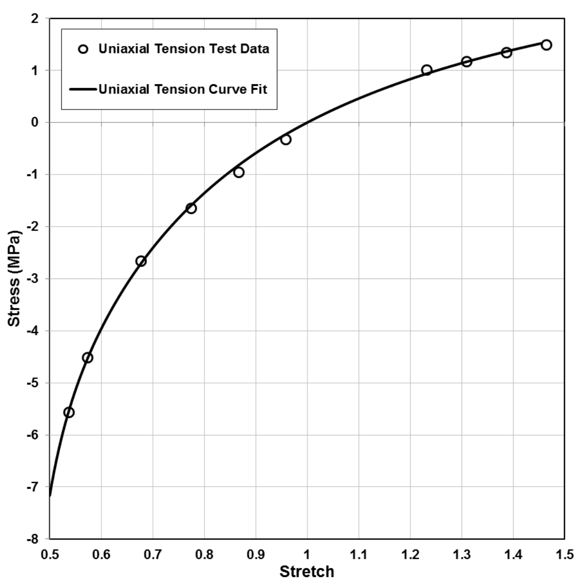

Figure 3: Experimental data [6] plotted against the proposed model for the quasi-static response of rubber at a strain-rate of 0.01 mm/mm/s.

uniaxial case. In order to do this, we first need to obtain the hyperelastic parameters for the case of quasistatic loading as seen in *Figure 3*. The parameters are given in *Table 3*, which we use to obtain the viscoelastic parameters in the next section [Bois (2003), Benson (2006) and Bois (2006)].

Table 3: Hyperelastic constants.

μ_1	μ_2	μ_3
-0.0105 MPa	-2.6469E6 MPa	2.8087E5 MPa
α_1	α_2	α_3
-5.1522	0.0005	0.0048

Table 4: Viscoelastic constants.

A	B	C	θ_1	θ_2
2.2655	-0.0253	0.5719	0.1791sec	0.0009sec

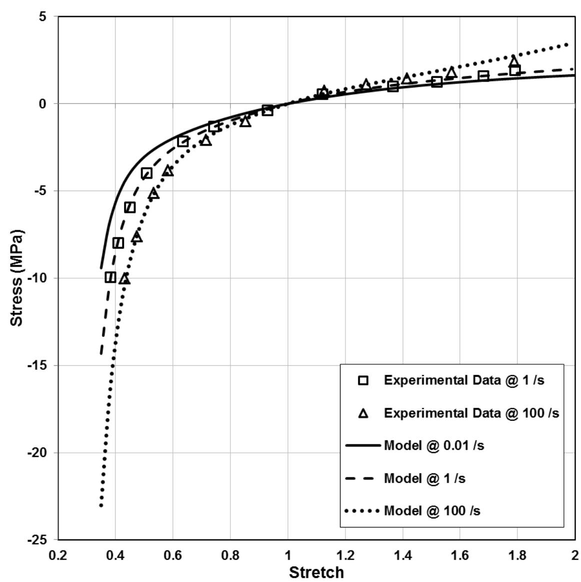

Figure 4: Experimental data [6] plotted against the proposed model for the dynamic response of rubber at a strain-rate of 0.01, 1.0 and 100.0 mm/mm/s.

Dynamic Response

After obtaining the hyperelastic parameters for the three-terms Ogden model, we find the parameters for the non-linear BKZ model while curve fitting our equation to both strain rates simultaneously, as given in *Figure 4*. The viscoelastic parameters, including the two different relaxation times, are given in *Table 4*.

3.3 Hysteresis

Quasi-static Response

Using the same set of data for the case of loading, as given by *Figure 3*, we find the unloading parameter for the case of hysteresis, for the tension and compression regions simultaneously. The experimental data and the model validation can be seen in *Figure 5*. The hysteresis material constant is given in *Table 5* and is given in relation to the damage variable η as:

$$\eta = \frac{\text{current stretch} - \text{maximum stretch}}{\alpha - \text{maximum stretch}}$$

Table 5: Hysteresis constant.

α
1.0037

Table 6: Hyperelastic constants for primary loading.

μ_1	μ_2	μ_3
1331.8 MPa	-1164.0 MPa	3.5757 MPa
α_1	α_2	α_3
-0.9159	-1.0676	2.9688

3.4 Mullins' effect

Primary Loading Response

Now for the case of Mullins effect, we consider another set of data, as shown in *Figure 6*. First, we have to characterize the primary hyperelastic response, thus obtaining the hyperelastic parameters as given in *Table 6*.

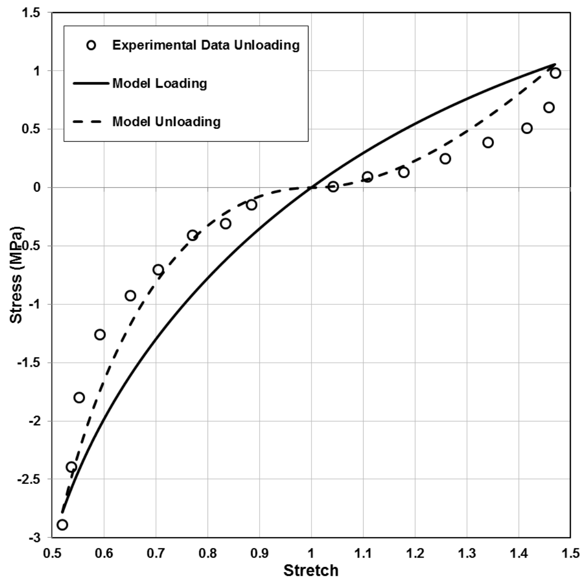

Figure 5: Experimental data [6] plotted against the proposed model for the unloading response of rubber using damage function at a strain-rate of 0.01 mm/mm/s.

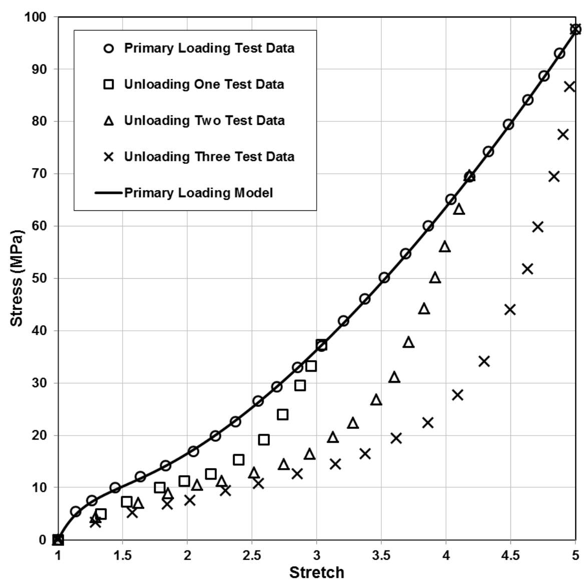

Figure 6: Experimental loading data [17] plotted against the hyperelastic three-term Ogden model for primary response of rubber compound.

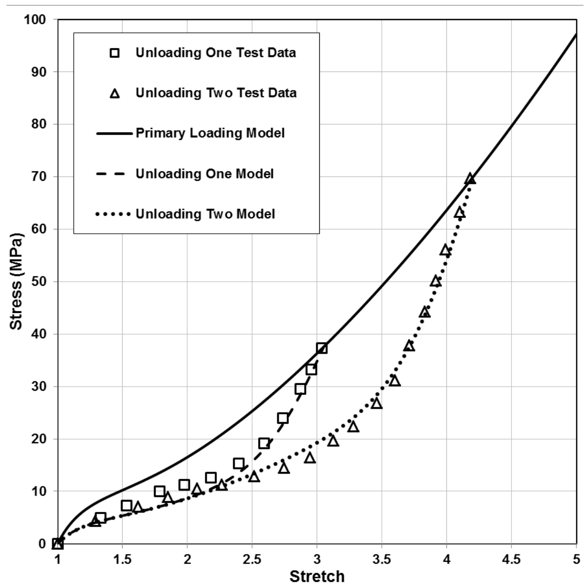

Figure 7: Experimental unloading data [17] plotted against the proposed model for Mullins' effect up to second maximum stretch.

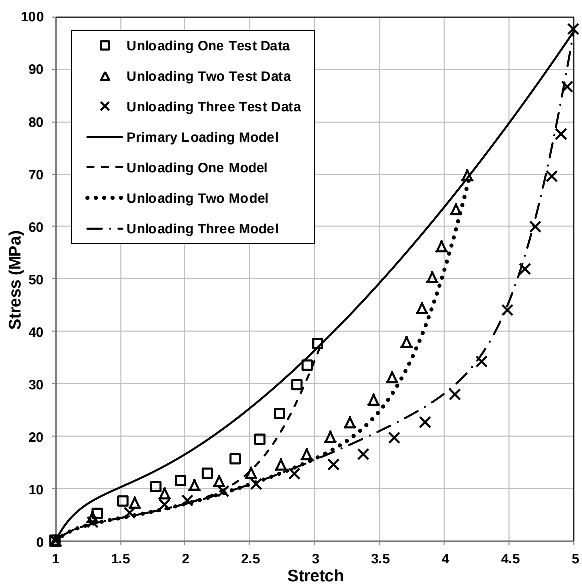

Figure 8: Experimental unloading data [17] plotted against the proposed model for Mullins' effect with third maximum stretch.

Unloading Response

Next, for unloading due to Mullins' effect, we have to find the parameters r and m, using data from all the points where unloading begins. We regard the first two points as our maximum stretch. The experimental data and the model can be seen in *Figure 7*. The parameters for the Mullins' effect are given in *Table 7*. We see that for the case of unloading using two points, we get a good fit but the model can also capture unloading from three points reasonably well. Therefore, for unloading including three maximum stretches, we again find the parameters r and m, using data from all three points where unloading begins. We regard these three points as our maximum stretch. The experimental data against the model can be seen in *Figure 8*. The parameters for the Mullins' effect now are given in *Table 8*.

Table 7: Mullins effect constants for unloading with second maximum stretch.

r	m
2.1000	71.5250

Table 8: Mullins effect constants for unloading with third maximum stretch.

r	m
1.7400	66.7640

4 Conclusion

A constitutive model is proposed to predict the response of rubber which is characterized by its' hyperelasticity, viscoelasticity, hysteresis and Mullins' effect. Based on experimental data, material parameters have been found and the constitutive models have been validated in a limited set of deformation modes. As seen in the results, one unified model can be used to capture the dynamic response of rubber-like polymers under different loading conditions with great accuracy. Since material is an intensive property, a constitutive model with a given set of parameters can be extended to a wide range of industrial applications.

References

Benson, D. J.; Du Bois, P. A.; Kolling, S. (2006): A simplified approach for strain-rate dependent hyperelastic materials with damage. *9th International LS-DYNA Users' Conference.*

Bernstein, B.; Kearsley, E. A.; Zapas, L. J. (1963): A study of stress relaxation with finite strain. *Transactions of the Society of Rheology,* vol. VII, pp. 391-410.

Bernstein, B.; Kearsley, E. A.; Zapas, L. J. (1965): Elastic stress-strain relations in perfect elastic fluids. *Transactions of the Society of Rheology,* pp. 27-39.

Bower, A. F. (2009): Applied Mechanics of Solids. *CRC Press.*

Calvo, B.; Pena, E. (2009): On modelling damage process in vaginal tissue. *Journal of Biomechanics,* vol. 42, pp. 642-651.

Dorfmann, A.; Ogden, R. W. (2003): A pseudo-elastic model for loading, partial unloading and reloading of particle-reinforced rubber. *International Journal of Solids and Structures,* vol. 40, pp. 2699-2714.

Du Bois, P. A. (2003): A simplified approach to the simulation of rubber-like materials under dynamic loading. *4th European LS-DYNA Users' Conference.*

Du Bois, P. A.; Kolling, S. (2006): Material behaviour of polymers under impact loading. *International Journal of Impact Engineering,* vol. 32, pp. 725-740.

Feng, W. W.; Hallquist, J. O. (2005): A failure criterion for polymers and soft biological materials. *5th European LS-DYNA Users' Conference.*

Feng, W. W.; Hallquist, J. O. (2007): Numerical modelling and biaxial tests for the Mullins' effect in rubber. *6th European LS-DYNA Users' Conference.*

Ferry, J. D. (1961): Viscoelastic Properties of Polymers. *Wiley Publications.*

Holzapfel, G. A. (2000): Nonlinear Solid Mechanics: A Continuum Approach for Engineering. *Wiley Publications.*

Hutter, K. (1993): Continuum Mechanics in Environmental Science and Geography. *Springer Publications.*

Miehe, C. (1995): Discontinuous and continuous damage evolution in Ogden-type large-strain elastic materials. *Eur. J. Mech., A/Solids,* vol. 14, no. 5, pp. 697-720.

Mullins, L. (1969): Softening of rubber by deformation. *Rubber Chemistry and Technology,* vol. 42, no. 1, pp. 339-362.

Ogden, R. W. (1972): Large deformation isotropic elasticity - on the correlation of theory and experiment for incompressible rubberlike solids. *Proc. R. Soc. London A.,* vol. 326, no. 1567, pp. 565-584.

Ogden, R. W.; Roxburgh; D. G. (1999): A pseudo-elastic model for the Mullins effect in filled rubber. *Proc. R. Soc. London A.,* vol. 455, no. 1988, pp. 2861-2877.

Ogden, R. W.; Saccomandi G.; Sgura, I. (2004): Fitting hyperelastic models to experimental data. *Computational Mechanics.*

Silva, H. N.; Soares, J. B.; Parente Jr., E.; Sousa1, P. C. (2008): Implementation of a Viscoelastic Constitutive Model Using the Object-Oriented Programming

Approach. *Tech Science Press ICCES*, vol. 7, no. 4, pp. 181-188.

Twizell, E. H.; Ogden, R. W. (1983): Non-linear optimization of the material constants in Ogden's stress-deformation function for incompressible isotropic elastic materials. *J. Austral. Math. Soc.,* ser. B 24, pp. 424-434.

Yang, L. M.; Shim, V. P. W.; Lim, C. T.; Law, P. H. (2004): A visco-hyperelastic constitutive model to characterize both tensile and compressive behavior of rubber. *Journal of Applied Polymer Science,* vol. 92, pp. 523–531.

Yang, L. M.; Shim, V. P. W.; Lim, C. T. (2000): A visco-hyperelastic approach to modelling the constitutive behavior of rubber. *International journal of impact engineering,* vol. 24, pp. 545-560.

Zapas, L. J. (1966): Viscoelastic behavior under large deformations. *Journal of Research of the National Bureau of Standards,* vol. 70A.